euspen's 18th International Conference & Exhibition, Venice, IT, June 2018
www.euspen.eu

Development of an X-ray radiograph simulator: from STL file to grey scale image

Lars Körner[1], Rong Su[1], Simon Lawes[1], Nicola Senin[1,2], Richard Leach[1]

[1]*Manufacturing Metrology Team, University of Nottingham, UK*
[2]*Department of Engineering, University of Perugia, Italy*

Lars.Korner@nottingham.ac.uk

Abstract
A polychromatic X-ray radiograph simulator has been developed to assist the structured exploration of the parameter space of X-ray computed tomography for dimensional and surface metrology. The simulator is capable of simulating polychromatic X-ray spectra, at user defined binning sets to produce radiographic images. This approach differs from existing simulation software in the use of a sparse matrix multiplication approach, between a geometry matrix and a voxel description, of the object to create both the cone beam and the focal spot geometries. Future work will aim to use this framework for the incorporation of scatter approximations.

X-ray computed tomography, simulation, metrology

1. Introduction

X-ray computed tomography (XCT) is a non-destructive imaging technique, which has recently gained interest as a metrological tool for both dimensional and surface metrology [1–3]. Whilst some of the characteristics of XCT, such as its non-contact volumetric measurement nature, are unique and desirable, the parameter space of XCT is large. Given the large number of variables to set for a XCT scan, simulation tools can assist both in finding optimum scanning parameters as well as exploring the parameter sensitivities [4].
One aspect often overlooked in XCT simulations is the role that the source focal spot can play in forming the projected image. The focal spot can be defined as the X-ray producing area of the target [5]. The focal spot has several properties of interest: size, shape, location and the location drift behaviour, and intensity. The properties of the focal spot have been discussed elsewhere, with respect to dimensional metrology [6,7], but also in depth during the early years of development of medical XCT [8–10]. Wagner et al. [8] showed that a noncircular and bimodal focal spot can cause artefacts around an imaged edge. The focal spot geometry needs to be considered when simulating radiographs, especially if the focal spot varies in both length and width. Current simulation tools can account for secondary spots [11], however, the complexity can increase, if different spectra are expected from the secondary spots. The main aim of the work reported here was to simulate the effect of different focal spot shapes.

2. The core of the simulation program

The development of the simulation model orginates on concepts of the forward projection engines as used in iterative reconstructions [12,13]. In order to include focal spot geometry in the simulation, the core of the simulation program was built on a voxel map of the simulated object. The cone beam effect is applied to the simulated object through the multiplication of a cone mask matrix. This matrix, which is sparse, describes the mapping of a pencil beam system to a cone beam system. In essence, the cone mask is a two-dimensional (2D) matrix of fractional values, which describes the relationship between the detector pixels and the voxel volume of the simulated object. In order to account for the shape and the size of the object, the focal spot is described through a normalised 2D matrix up to a maximum size of 512 by 512 elements. The shape of the focal spot is included by evaluating the cone mask for each non-zero element of the focal spot descriptor. Hence, a focal spot adjusted cone mask is created (figure 1). To obtain the final voxel volume, the focal spot cone mask is multiplied with each voxel layer through the magnification axis.
The Beer-Lambert law describes quantitatively the change of intensity of a parallel beam of photons travelling through a material with a mass attenuation coefficient $\mu(E)$:

$$I(x) = I_0 \, e^{-\mu(E)\,x}, \tag{1}$$

where I_0 denotes the initial intensity of the parallel beam, $I(x)$ is the intensity after having travelled the length x through the material and E is the energy of the photon. Equation (1) is evaluated for the desired binning of the spectrum for both the object evaluation and the calculation of the filtration.
In order to obtain the 2D radiograph, the voxel volume is reduced through summation to a 2D matrix, followed by an evaluation of equation (1), and estimating the detector response through the mass attenuation profile of the scintillating material.

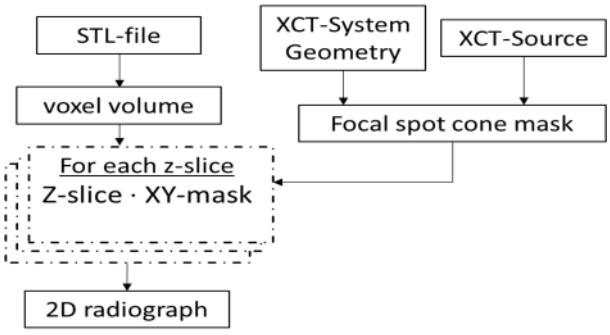

Figure 1. Simplified process map of the simulation program.

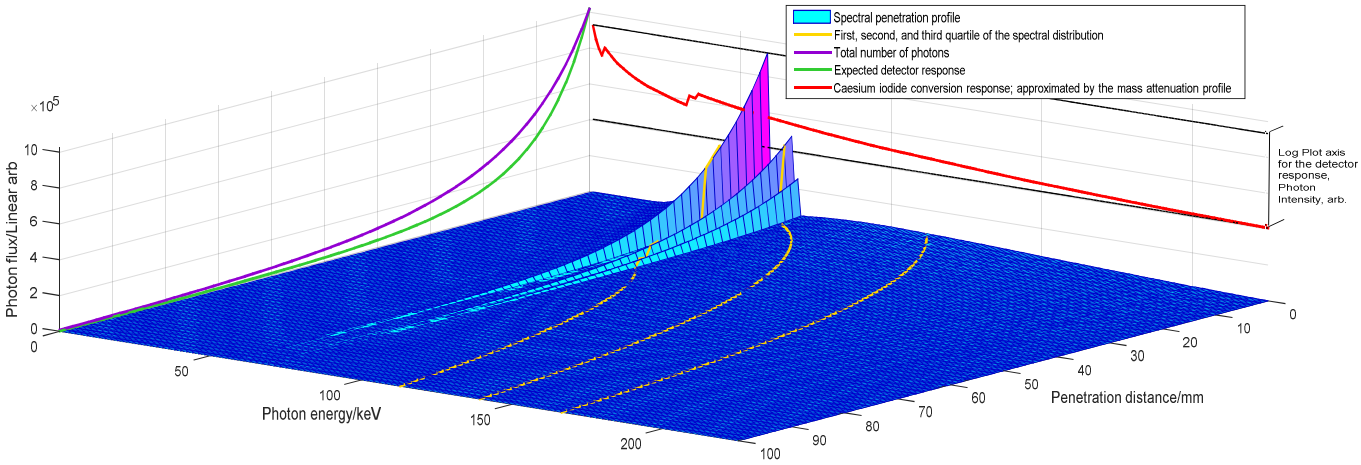

Figure 2. Penetration profile of an Al object by an X-ray spectrum produced from a 225 kV accelerating voltage and a tungsten target.

3. Simulation results

The infographic in figure 2 demonstrates the polychromatic capacity of the simulation software. Figure 2 shows the change of the spectrum as the X-rays travel through aluminium, and the initial spectrum is based on tungsten with an assumed self-filtration of 5 µm of tungsten followed by a filter of 500 µm of beryllium, as calculated by the X-ray simulation software. The spectrum calculations are based on [10]. The blue surface plot shows the change in spectrum, and the red line shows the simplified detector response model in respect to the X-ray spectrum. The green line shows the expected detector grey level reading, while the purple line shows the relative photon flux at each distance through the material.

Figure 3 shows a comparison between a simulation and an experimental 2D radiograph. The experimental 2D radiograph was captured using the average of 32 images at an acceleration voltage of 225 kV at 10 W and an exposure of 4 s. The tube used is a Nikon 225 kV tube, with a tungsten reflection target, and an added filtration of 1 mm copper. Figure 3c) is a line plot showing the 16 bit grey level reading of the detector at the central row, approximately the location of the iso-ray for the physical system. The experimental radiograph shows additional side slopes at the edges of the cylinder, which cannot be seen in the simulated radiograph. This is not expected to be due to the focal spot and is most likely due to scattering. Also, the simulated shape of cylinder function differs. This may be due to wrongly estimated material coefficients, as the simulation used elemental aluminium, whereas the real part is an engineering alloy based on aluminium. The apparent difference in size of the projected cylinder, as seen in figure 3, was traced back to the inappropriate, off-centre fixturing of the cylinder which led to an incorrect determination of the magnification in the comparison.

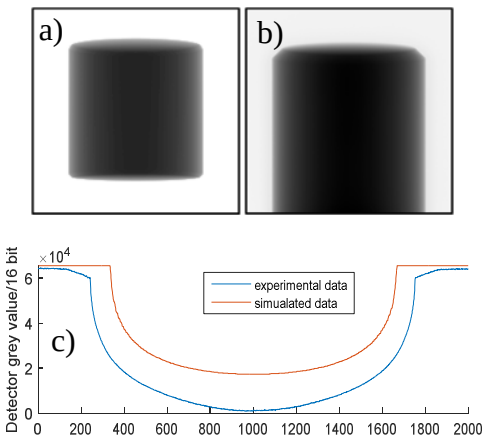

Figure 3. a) Simulated image of a 30 mm cylinder, b) experimental 2D radiograph, and c) showing the grey level reading for both experimental and simulated central slice

The current implementation is non-optimised and is written in a non-compiled language; the time on an Intel Xeon CPU E5-1620 v3 to simulate a radiograph with 250 energy evaluations onto a 2000 by 2000 pixel detector is approximately 3 mins.

4. Future work, summary and conclusion

A polychromatic X-ray simulator has been presented, which uses a geometric modelling approach to account for the shape of the focal spot and the cone beam geometry. The attenuation mapping compares well against experimental 2D radiographs, although a detailed calibration of the simulator against the physical XCT system is still required to eliminate a number of error sources. Currently the effects of scattering, flux of the x-ray source, detector noise or exposure time have not been accounted for in the simulation, but future plans include the characterisation of the x-ray source and detector such that the simulation program can estimate the expected levels of noise.

Acknowledgements

The authors would like to acknowledge funding from the following grants of the EPSRC: EP/101534X/1 and EP/M008983/1.

References

[1] Kruth J P, Bartscher M, Carmignato S, Schmitt R, De Chiffre L and Weckenmann A 2011 *Ann. CIRP* **60** 821–42

[2] Townsend A, Pagani L, Scott P and Blunt L 2017 *Precis. Eng.* **48** 254–64

[3] Carmignato S, Dewulf W and Leach R 2018 *Industrial X-Ray Computed Tomography* (Springer International Publishing)

[4]Thompson A, Senin N, Maskery I and Leach R K 2017 *Dimensional X-ray Computed Tomography*, Coventry, UK

[5] European Committee for Standardization Non-destructive testing — EN 12543-2008 Characteristics of focal spots in industrial X-ray systems for use in nondestructive testing Part 2: Pinhole camera radiographic method

[6] Flay N, Sun W, Brown S, Leach R K and Blumensath T 2015 *Digit. Ind. Radiol. Comput. Tomogr.* 22–5

[7] Bavendiek K, Ewert U, Riedo A, Heike U and Zscherpel U 2012 *18th World Conf. Nondestruct. Test.* 16–20

[8] Wagner R F, Weaver K E, Denny E W and Bostrom R G *Med. Phys.* **1** 11–24

[9] Tennet W 1970 *The diagnostic X-ray tube* (Surrey: Mullard Educational Service)

[10] Barret H and Swindell W 1981 *Radiological imaging the theory of image formation, detection, and processing Volume 1* (New York: Academic Press)

[11] Dhaene J, Pauwels E, De Schryver T, De Muynck A, Dierick M and Van Hoorebeke L 2015 *Nucl. Instruments Methods Phys. Res. Sect. B Beam Interact. with Mater. Atoms* **342** 170–8

[12] Hsieh J 2009 Computed Tomography (Washington: SPIE)

[13] Beister M, Kolditz D and Kalender 2012 W Phys. Medica **28** 94–108